Concurrent OH imager and sodium temperature/wind lidar observation of a mesopause region undular bore event over Fort Collins/Platteville, Colorado

C. Y. She, Tao Li, Bifford P. Williams, and Tao Yuan
Department of Physics, Colorado State University, Fort Collins, Colorado, USA

R. H. Picard
Air Force Research Laboratory, Hanscom AFB, Massachusetts, USA

Received 8 March 2004; revised 15 June 2004; accepted 7 September 2004; published 27 November 2004.

[1] We reported the observation of a mesospheric front with the properties of an undular bore by an OH imager, over the Fort Collins/Platteville area on 6/7 October 2002. Unlike the earlier bore observations, a Na lidar capable of measuring mesopause region temperature, zonal, and meridional winds was in operation concurrently. The lidar data confirm, for the first time, the existence of a collocated temperature inversion layer to serve as the ducting region for bore propagation, as required by the simple theory proposed by Dewan and Picard 6 years ago. In addition, the lidar data in principle provide sufficient information for the determination of all parameters of the bore as suggested by the simple theory. The parameters so determined are compared to two bores previously studied. Like the earlier cases, the horizontal wavelength estimated from the theory is in good agreement with the observation. The lifetime of this undular bore, ~120 min, was considerably shorter than the other two. Continued lidar observation after the bore event reveals that the ducting region may be controlled by a long-period wave, most likely related to a semidiurnal tide, and that atmospheric dynamic instability occurs simultaneously with the destruction of the wave train associated with the bore. It is possible that this constitutes, for the first time, the observation of the transition from an undular to a turbulent, or foaming, internal bore predicted by the theory. *INDEX TERMS:* 3332 Meteorology and Atmospheric Dynamics: Mesospheric dynamics; 0310 Atmospheric Composition and Structure: Airglow and aurora; 0394 Atmospheric Composition and Structure: Instruments and techniques; 3384 Meteorology and Atmospheric Dynamics: Waves and tides; *KEYWORDS:* airglow, mesospheric bore, sodium lidar

Citation: She, C. Y., T. Li, B. P. Williams, T. Yuan, and R. H. Picard (2004), Concurrent OH imager and sodium temperature/wind lidar observation of a mesopause region undular bore event over Fort Collins/Platteville, Colorado, *J. Geophys. Res.*, *109*, D22107, doi:10.1029/2004JD004742.

1. Introduction

[2] *Taylor et al.* [1995] reported a "spectacular gravity wave event" from their four-color airglow imager observation in Hawaii in 1993. This event was characterized by a sharp airglow front traveling for hours at constant velocity. There was a large change in brightness across the front and waves behind it that traveled at the frontal speed. There was also a contrast reversal between the images of the lower-altitude airglow layers (OH and Na) and the higher-lying layers (O_2 atmospheric, $O(^1S)$ green line). Adapting the theory of river channel bore formation and propagation [e.g., *Lighthill*, 1978], *Dewan and Picard* [1998] identified this event as an internal undular bore in the mesosphere, and developed a simple model for bore propagation into a ducting region, which allowed the determination of several parameters including bore speed U, buoyancy-corrected gravitational acceleration g', mean horizontal wavelength λ_h and amplitude a of the associated waves, and bore wave generation rate dW/dt. These bore properties are expressed in terms of unperturbed duct depth h_0 and the increased duct depth h_1 behind the bore front, which defines the normalized bore amplitude β. In this paper, they also proposed that the duct could be formed by a stable atmospheric region associated with temperature inversion layer. In a follow up paper [*Dewan and Picard*, 2001], they suggested that the critical-level interaction, previously proposed as a source of inversion layers [*Huang et al.*, 1998, 2002], was also the source of the body force that provided the transient fluid acceleration to form the bore. Obviously, in order to verify their suggestion of the bore-ducting mechanism, a collocated temperature inversion must be observed in nature.

[3] Strong but indirect evidence associating the existence of temperature inversion and bore propagation was published in a recent paper by *Smith et al.* [2003]. An unusually

Copyright 2004 by the American Geophysical Union.
0148-0227/04/2004JD004742

clear spectacular internal undular bore, observable by naked eye was recorded at McDonald Observatory (MDO) in Texas (30.7N, 104W) on the night of 13/14 November 1999. Coincidentally, the Colorado State Na lidar was observing the same night some 1100 km to the north. A large temperature inversion of ~50 K was observed ~6 hours prior to the passage of this highly sinusoidal "text book like" undular bore over MDO, consistent with the observed speed of southward bore propagation at ~60 ms^{-1}. In this paper, we report what is believed to be the first observation of internal undular bore with collocated and simultaneous lidar observation of temperature inversion. Since the lidar is capable of measuring mesopause region temperature, zonal and meridional winds, not only can we verify the existence of a duct-forming temperature inversion layer, but we can also determine the key parameters of the observed bore directly from observational data. Lidar data also suggest, again for the first time, that dynamic instability is associated with the demise of the bore's associated waves, and we may have the first observation of a bore changing its form from undular to turbulent.

2. Observation

[4] The facility for ground-based optical observation in the Fort Collins/Platteville (FC/P) area was deployed in 2001 as a part of the NASA/NSF TIMED/CEDAR collaboration. The main instrumentation consists of an all-sky imager and a two-beam narrowband sodium lidar. The all-sky imager is the contribution of Kieffaber and Peterson from Whitworth College, WA [*Peterson and Kieffaber*, 1973], modernized to acquire one image every 2 min automatically at night. At present, only the OH channel is used and routine data acquisition began in September 2001. To preserve the acquisition rate, a second imager with an OI channel is being considered for future deployment as an alternative to time sharing the current imager. The two-beam narrowband sodium lidar was upgraded from the single-beam temperature only lidar to the current configuration, capable of measuring mesopause region temperature, zonal and meridional winds simultaneously on a 24-hour continuous basis, weather permitting [*She*, 2004]. The current mode of operation began data acquisition in May 2002 with two beams pointing 30° from zenith, one to the east and the other to the north. The lidar measurement uncertainty depends on photon noise, which may be reduced at the expense of temporal and spatial resolution. Our typical analysis with nighttime data uses 2 km vertical smoothing and 1 hour temporal integration, giving a measurement uncertainty of ~0.5 K and ~2 m/s respectively for temperature and horizontal wind at the peak of the Na layer. The signal-to-noise of nighttime measurements is good enough to allow calculation of vertical profiles of mesopause region temperature and wind with 30-min or 15-min temporal resolution, which are used in the discussions below.

[5] The locations of both instruments are shown in Figure 1. At the center marked Platteville is the location of the all-sky imager with a 65° half field of view circled in by a solid line. The site of the two-beam lidar is marked as CSU lidar, with the respective viewing volumes in the mesopause region mar CSU 30E and CSU 30N. In the mesopause region, the separation between these two points is ~70 km and the lidar beam diameter is ~100 m.

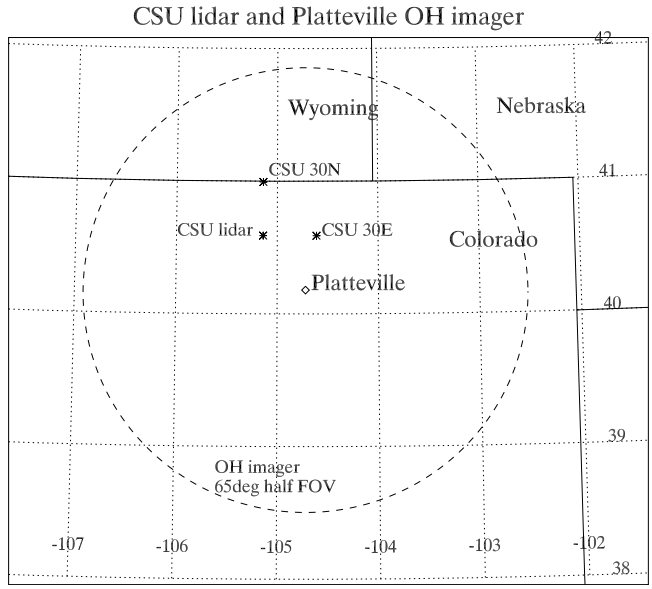

Figure 1. Locations of Platteville OH imager, CSU Na lidar, and its 30° off zenith north and east beam viewing positions in the mesopause region.

[6] The lidar was in operation between 0200 and 1200 UT in the night of 6/7 October 2002. Cloudy conditions between 2.5 and 5.0,UT made optical observation impossible. Nonetheless, the presence of a brief observation at ~2.0,UT reveals that a strong temperature inversion exists at the OH layer height between 2.0 and 9.0,UT. Fortunately, the entire bore event observed by the imager lasts from 0510 to 0730,UT, when clear sky prevailed to allow lidar operation throughout the observed lifetime of the bore. As will be discussed later, the observed temperature inversion appears to be associated with a long-period wave, presumably related to the semidiurnal tide. The mesosphere and lower thermosphere (MLT) region was very active this night. Viewing the all-sky imager movie, in addition to the bore event we are reporting, we detected another bore-like event coming in from the upper right corner between 0900 and 0935 UT, as well as small-scale waves after 0830 UT, south of Platteville, attributable possibly to Kelvin-Helmholtz (KH) instability. Since most of these events occur outside the viewing volume of the two-beam lidar, we will concentrate on the bore event between 0510 and 0730 UT. To examine this bore event in more detail, we show the OH difference images at selected snap shots with a 5° × 5° latitude-longitude view. Nine images at about 0509, 0536, 0555, 0603, 0614, 0643, 0653, 0710, 0731 UT, are shown in Figure 2, corresponding to (Figure 2a) bore onset, (Figure 2b) maturity of undulation, (Figure 2c) front propagation to the east beam, (Figure 2d) front between two lidar beams, (Figure 2e) front propagation to the north beam, (Figure 2f) bore beginning to lose undulations, (Figure 2g) disintegration of bore undulation, (Figure 2h) appearance of a single propagating bore front followed by turbulence (foaming wave segments) or of a turbulent (foaming) bore, and (Figure 2i) further weakening

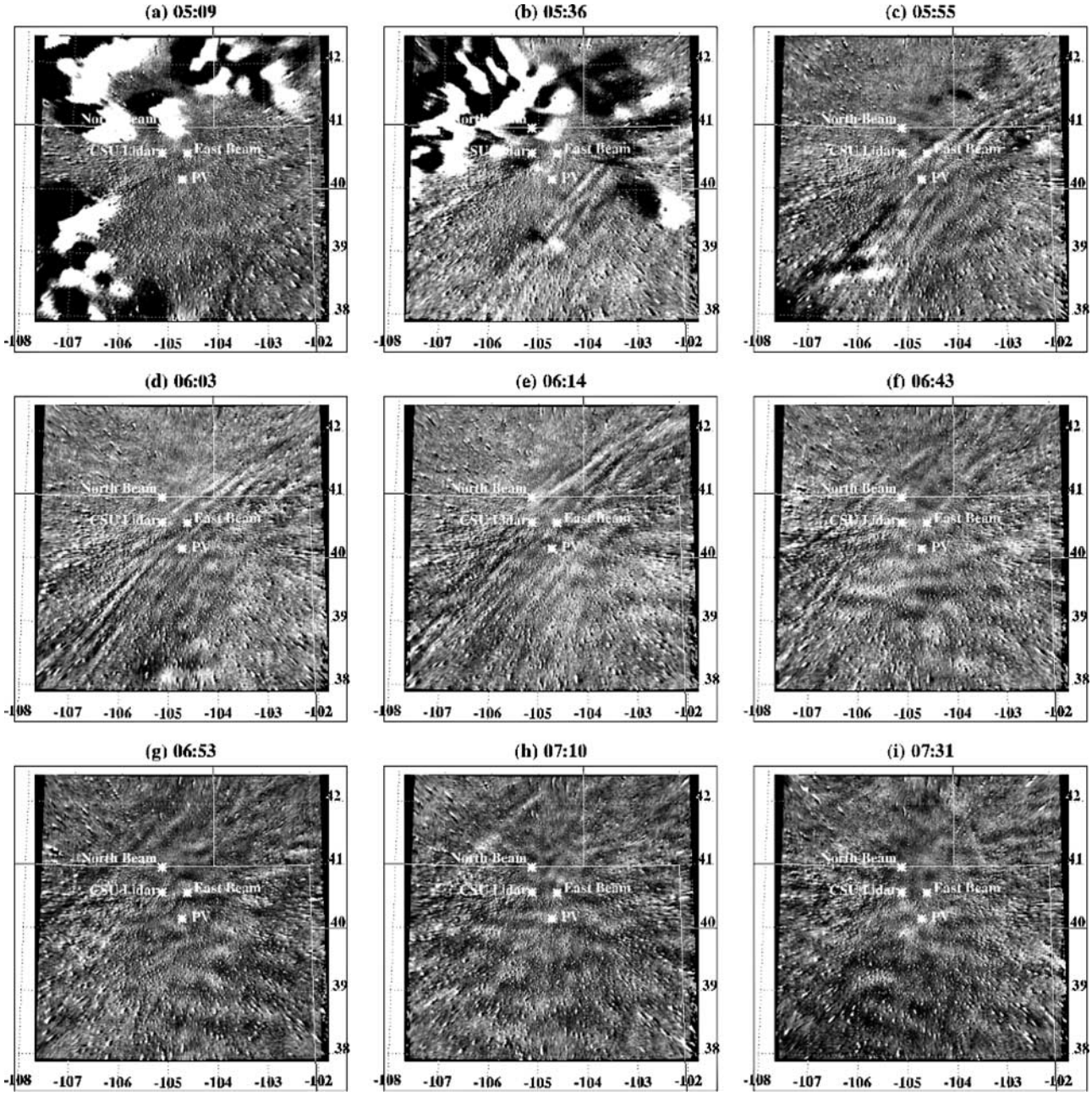

Figure 2. OH imager snap shots of flat-fielded difference images restricted to within 5° × 5° of Platteville, CO, taken on the night of 6/7 October 2002 at about 0509, 0536, 0555, 0603, 0614, 0643, 0653, 0710, and 0731 UT, showing the (a) bore onset, (b) maturity, (c) front propagation to the east beam, (d) front between two lidar beams, (e) front propagation to the north beam, (f) bore beginning to lose undulations, (g) disintegration of bore undulation, (h) appearance of a single propagating bore front followed by turbulence (foaming wave segments) or of a turbulent (foaming) bore, and (i) further weakening of the bore. The difference image is constructed by subtracting the earlier image from the current one.

of the bore. At 0603 we observed maximum contrast on undulations with a total of 4 or 5 crests including the bore front. At 0614, as it passed the north beam, the front crest became dimmer and it began to merge into the background. At 0710 when turbulent bore was first seen, there exists a hint of short wavelength ripple-type structure centered near 100 km east of the line connecting "CSU lidar" and "CSU 30N." The lifetime of ndular phase of this bore is ~120 min; since the observed bore speed is ~74 m/s, it traveled a total distance of ~530 km during this time.

3. Determination of Bore Parameters

[7] One salient merit of this first concurrent observation of a bore event by OH imager and a narrowband Na lidar, capable of measuring temperature and zonal and meridional

Table 1. Comparison on the Parameters of Three Undular Bore Events

Parameters of Undular Bore	h_0/h_1, km ($-u_0'/-u_1'$, m/s)	β	g', m/s^2	U, m/s	dW/dt, hr^{-1}	a, km	λ_h, km
1993 Hawaii	2.7/3.5	0.3	1.4	76	2.8	0.6	19
1999 MDO	3.0/3.9	0.3	0.91	60.2	1.5	0.68	30
2002 FC/P-0 at 87 km	3.0/3.3 (95.3/86.3)	0.10	2.6	74	1.3	0.19	31
2002 FC/P-1 at 87 km	2.7/3.0 (95.3/86.3)	0.11	2.9	74	1.6	0.19	27

winds, lies in its capability for determining the key parameters describing the undular bore exclusively from observational data without using information from atmospheric models. To appreciate this possibility, we recall the simple model of *Lighthill* [1978] adapted to the MLT by *Dewan and Picard* [1998], in which they consider a bore event with a (phase) speed U propagating within a stationary ducting region with the undisturbed depth or thickness h_0. The disturbance resulting from the "hydraulic" jump after the bore increases the duct thickness to h_1. The model must be modified to allow for the presence of a horizontally uniform background wind along the bore propagation direction that the lidar measures. The presence of such a background flow was not considered in the work of *Dewan and Picard* [1998] or in the work of *Lighthill* [1978]. We briefly summarize the result of such an extension of the theory here. In the observer's rest frame the wind component u_0 in front of the bore is the coaligned (with bore's wave vector) background wind $\bar{u}$, that is $u_0 = \bar{u}$, while behind the bore the coaligned wind speed u_1 includes a small velocity in the bore direction in addition to $\bar{u}$. Note that a bore is largely a phase motion rather than a fluid flow, so that we would expect u_0 and u_1 to be much smaller than the bore (phase) speed U. In fact, without a background wind $\bar{u}$, $u_0 = 0$ while u_1 is small and positive, or in the bore propagation direction. In the frame moving with the bore, u_0 and u_1 transform to $u_0' = \bar{u} - U$ and $u_1' = u_1 - U$, which are both negative, and conservation of mass results in a simple relation between these speeds and the duct depths, h_0 and h_1. The normalize bore amplitude β [*Lighthill*, 1978] may then be written as

$$\beta = \frac{h_1 - h_0}{h_0} = \frac{u_0' - u_1'}{u_1'} \text{ with } h_1 = \frac{u_0' h_0}{u_1'}. \quad (1)$$

[8] There is a necessary loss of energy by the bore across the hydraulic jump. This energy ideally is transmitted backward forming a series of phase-locked waves propagating with the bore (front). For channel bores, if $\beta < 0.3$, the waves following the bore are stable, and the disturbance is called undular bore. When $\beta > 0.3$, the waves will break leading to a propagating bore with a trailing region of turbulence, and this disturbance is called a turbulence (or foaming) bore. In addition, in an internal bore, energy may also be leaked out of the ducting region. Therefore it is possible that an internal bore with $\beta > 0.3$ could remain undular. For a weak undular bore ($\beta \ll 1$), following *Smith et al.* [2003] and *Dewan and Picard* [1998], the horizontal wavelength of the undular waves, λ_h, the wave amplitude, a, and the index of nonlinearity, c_n, may be expressed as

$$\lambda_h = \frac{2\pi h_1}{} \sqrt{\frac{2h_0}{h_1 - h_0}}, \quad (2)$$

$$a = \frac{1}{\sqrt{3}} \frac{h_1(h_1 - h_0)}{h_0}, \quad (3)$$

$$c_n = \frac{a\lambda_h^2}{h_1^3} = \frac{8\pi^2}{3^{2.5}} = 5.1. \quad (4)$$

Note that in the approximation of the Lighthill theory, c_n is a universal constant.

[9] In determining these parameters for the bore observed on 10 October 1993 by *Taylor et al.* [1995], *Dewan and Picard* [1998] used the pressure of the U.S. 1976 Standard Atmosphere and temperature from a collocated lidar measurement on a different date, 21 October 1993, to estimate the parameter g' (gravity acceleration multiply or corrected by fractional change in potential temperature from h_0 to h_1), from which the parameters U, h_1 and h_0 were calculated. The values of h_0 and h_1 are then adjusted to yield the observed U and λ_h. *Dewan and Picard* [1998] also confirm that their resulting value of $h_1 - h_0 = 0.8$ km is correct from the temperature rise of 8–12 K seen by a collocated OH temperature measurement [*Taylor et al.*, 1995]. In analyzing the bore observed at MDO, *Smith et al.* [2003] used a similar method to determine g'. With the temperature inversion profile measured 1100 km north, they determined h_0. They assumed a $\beta = 0.3$, giving $h_1 = 3.9$. These values were used for the 1999 MDO bore entry in Table 1. Alternatively they could have used the OH temperature change before and after bore passage of 5 K, measured by a OH temperature mapper in nearby Albuquerque, to estimate the height change, $h_1 - h_0 \sim 0.5$ km, and then parameters a and β. In our case we can determine g' from the bore speed, using *Dewan and Picard* [1998, equation (12)], suitably modified for the presence of a background wind

$$(U - \bar{u})^2 = \left(-u_0'\right)^2 = \frac{1}{2} g'(h_0 + h_1) \frac{h_1}{h_0}. \quad (5)$$

[10] Since the mesopause region temperature, zonal and meridional winds are measured by the two-beam Na lidar, we should be able to determine the wind speed ahead of (u_0) and behind (u_1) the bore in addition to the unperturbed ducting depth, h_0, from temperature profile. Because the bore travels from southeast to northwest at 135° ± 4°, it passes the east lidar beam first at 0555 and the north beam later at 0614. To describe the atmospheric condition in the region, we use the averaged temperature measured by the two beams, and zonal wind measured by the east beam and meridional wind by the north beam. To illustrate the state of the atmosphere while the bore undulation are in the area of lidar beams, we plot the observed profiles of 15-min averaged temperature, and associated Brunt-Vaisala fre-

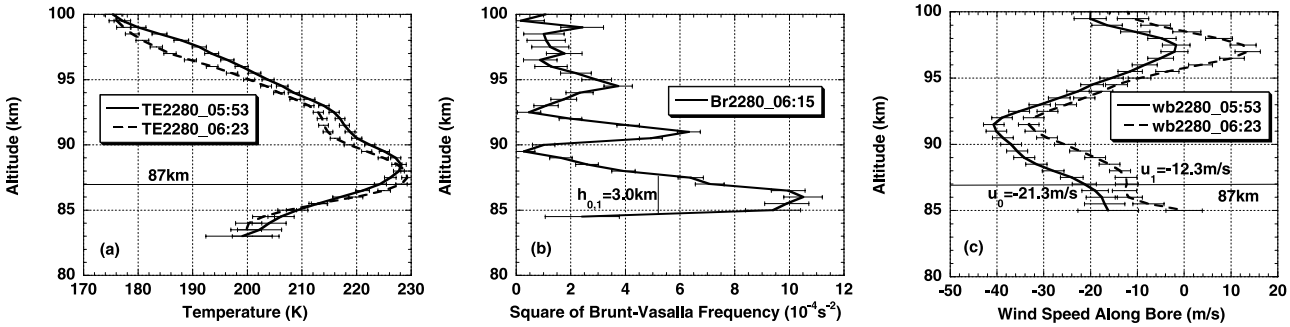

Figure 3. (a) Profiles of 15-min averaged, two-beam combined temperature (b) and associated Brunt-Vaisala frequency square, and (c) wind speed in the direction of bore propagation.

quency squared, N^2, as well as the wind speed along the bore propagation direction, centered at selected times in Figures 3a, 3b, and 3c, respectively. The spatial resolution of these profiles is 2 km. In Figure 3a, temperature profiles before and after the bore front passed the region at 0553 UT and 0623 UT are shown. A ~30 K temperature inversion with maximum at 88 km is clearly seen in both temperature profiles, defining a ducting region. At the altitude of 87 km, the nominal OH layer height [*She and Lowe*, 1998], the temperature at 0623 UT is higher than that at 0553 UT by 4 ± 1.4 K. The depth of the ducting region may be determined from the full width at half maximum in the N^2 profile, giving $h_0 \sim 3.0$ km as marked in Figure 3b. The reason we show the N^2 profile here at 0623 UT, a time midway between the times for the profiles in Figure 3a, is that within the spatial resolution and the error bars as shown, the N^2 profiles at the three times are essentially the same. In other words, the lidar measurements are incapable of resolving the difference between h_0 and h_1. In this sense, the FWHM measured in Figure 3b could be taken as either h_0 or h_1, allowing two possible and similar calculations of bore parameters, to be designated as 2002FC/P-0 and 2002FC/P-1. Since both zonal and meridional wind components are measured, we have calculated the wind speed along the direction of bore propagation (from southeast to northwest) as a function of time. The profiles of the wind speed along bore propagation, before (at 0553 UT) and after (at 0623 UT) the bore (front), are shown in Figure 3c. At 87 km they are −21.3 m/s and −12.3 m/s respectively. Since the bore speed is U = 74 m/s, the wind speeds relative to the bore are $u_0' = -95.3$ m/s and $u_1' = -86.3$ m/s, respectively. Using $h_0 = 3.0$ km and equation (1), we obtained $h_1 = 3.3$ km, and $\beta = 0.10$ for FC/P-0. The horizontal wavelength of the undulation, and bore amplitude are then calculated from equations (2), and (3), respectively, to be $\lambda_h = 31$ km, and a = 0.19. For FC/P-1, we use $h_1 = 3.0$ km, the same procedure gives rise to $h_0 = 2.7$ km, $\beta = 0.11$, $\lambda_h = 27$ km and a = 0.19. The index of nonlinear interaction, c_n is a universal constant for the simple model. In addition, we find from the expression relating bore speed to buoyant acceleration, equation (5), that $g' = 2.6$ m/s^2 and 2.9 m/s^2, respectively for FC/P0 and FC/P1.

[11] These bore parameters, designated as 2002 FC/P (at 87 km), may be compared to those of the 1993 Hawaii bore and 1999 MDO bore in Table 1. Notice that climatological values, educated guess noncollocated or nonsimultaneous data were required for the characterization of the 1993 [*Dewan and Picard*, 1998] and the 1999 [*Smith et al.*, 2003] bores, leading to more than one possible set of values. The values given in the table for these two bore events are the best choices of the authors. The failure of lidar to determine the difference between the duct depth before and after the "jump" admits two similar alternatives; they both are listed in Table 1 for comparison. Note that the values of U, u_o' and u_1' in the table for the FC/P events are measured, and all other parameters are estimated from the simple theory. The third entry from right in Table 1, dW/dt, is the rate at which full waves generated in the undulation wave train per hour. The bore must lose energy, and an undular bore does this by adding waves continuously as time goes on. From the required loss rate, the rate at which waves are added can be estimated. We will discuss the comparison and ramification of dW/dt and other quantities the section below.

4. Discussion

[12] Despite the fact that *Dewan and Picard* [1998] and *Smith et al.* [2003] used the maximum strength for an undular bore and assumed $\beta = 0.3$, the comparison shown in Table 1 clearly suggested that the undular bore we report here is relatively weak in comparison, with more than ~65% smaller values for a = 0.19 km and $\beta \sim 0.10$. The estimated horizontal wavelength, λ_h, is one parameter that may be checked with observation. With the best choices of parameters, good agreement was obtained in the cases of 1993 Hawaii and 1999 MDO bores. Without adjustment, we estimated $\lambda_h = 30.9$ km and 26.7 km for FC/P-0 and FC/P-1, respectively. The measured value of λ_h, using the waves in imager photo at 0555 (Figure 2c), 0603 and 0614 (Figure 2d), ranges between 24 km and 30 km, with the wavelength closer to the laser beams being ~27 km. Unlike the 1999 MDO bore, there is a spread in the waves associated with the 2002 FC/P bore, because the FC/P bore's waves are much less monochromatic. In view of this uncertainty, we consider the agreement to be good. The ideal dissipation rate, dW/dt, the third column from right in Table 1 is another parameter that may in principle be checked by observation, though it may be difficult in practice. The estimated value for the FC/P bore reported here is smaller than or comparable to the MDO bore. A discussion of the validity of this estimation for the FC/P bore is in order.

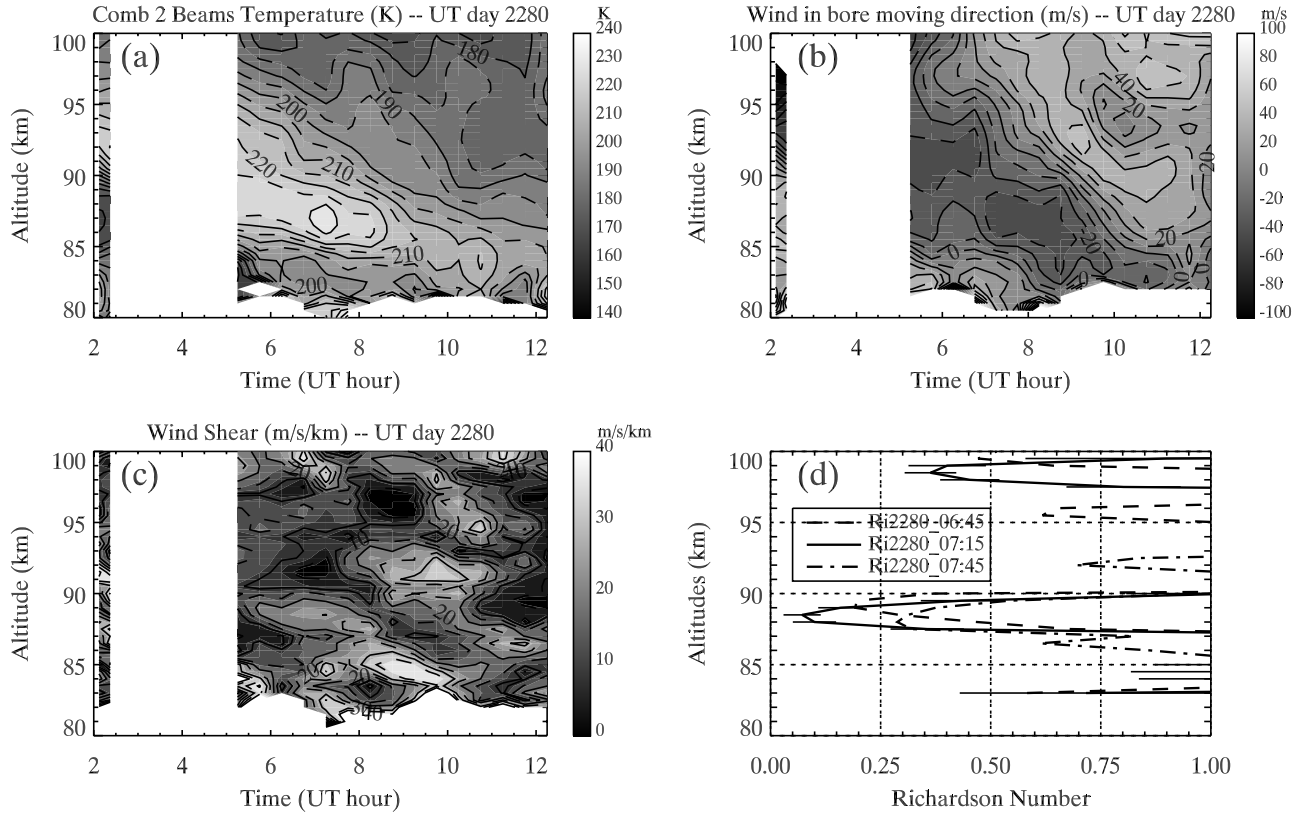

Figure 4. Contour plots of (a) temperature, (b) wind speed along bore propagation direction, and (c) the magnitude of vertical gradient of horizontal wind throughout the night of 6/7 October 2002. These contours are based on respective 30-min averages profiles. (d) Plots of Richardson number profiles at 30-min interval centered at different times. See color version of this figure at back of this issue.

[13] Assuming no energy leakage from the duct, *Dewan and Picard* [1998] estimated the rate of adding waves to the bore's tailing wave train as

$$\frac{dW}{dt} = \frac{3.6(U - \bar{u})(h_1 - h_0)^3}{2a^2 \lambda_h h_1} \left(hr^{-1}\right), \qquad (6)$$

where lengths are in km and velocity in m/s. As stated earlier, the 1999 MDO bore is unusually clear and highly sinusoidal. It appears to have a much longer lifetime than the 1993 or the 2002 bore. At the end of observation period, the number of visible crests in the MDO bore is still increasing, making it possible to determine the dissipation rate as defined in equation (6) experimentally. Indeed, the observed and estimated rates are very similar for the MDO bore [*Smith et al.*, 2003]. However, this rate was not measured for the 1993 Hawaii bore, but only estimated from the theory. Using the bore parameters, depending on the choices of h_0, we calculated the dissipation rate to be 1.3 or 1.6 per hour for the 2002 FC/P bore. Since there were only a few very clear undulation wave crests, varying between one and four, the observed rate unfortunately cannot be determined accurately. Though there were six to seven crests on the left side of the bore, their propagation is somewhat obscured. For the clear undulation wave crests, the number ranges from 1 to 4 between 0510 to 0603, and they disappeared altoge ~0710,UT. The bore's waves enter into the field-of-view already formed; their origin was not observed.

[14] In addition, we note that equation (6) deals only with the rate at which the number of wave crests increases. However, their disappearance rate is also important for the bore we studied here since the wave crests are being destroyed toward the end of the observation period. The problem is that equation (6) results from a steady state, which requires an ideal, highly sinusoidal and long-lived bore, such as the 1999 MDO bore, for its validation. On the other hand, the bore event reported here has a relatively short lifetime of ~120 min from cradle to grave as far as observable undulations are concerned. A theory dealing with the transient phase of the undular bore generation and demise is clearly needed. Such a theory is under development (R. H. Piccard, private communication, 2004). In this case, one expects the interaction and energy exchange with the background atmosphere to be more important and more complicated. The index of nonlinear interaction, c_n, should no longer be a universal constant for the transient case, where nonlinear interaction could well be either more pronounce or less pronounce depending on circumstances.

[15] To carry on further discussion, we show three lidar contours in Figure 4: plots of temperature, wind speed along the direction of bore propagation, and the magnitude of vertical gradient of horizontal wind throughout the night of

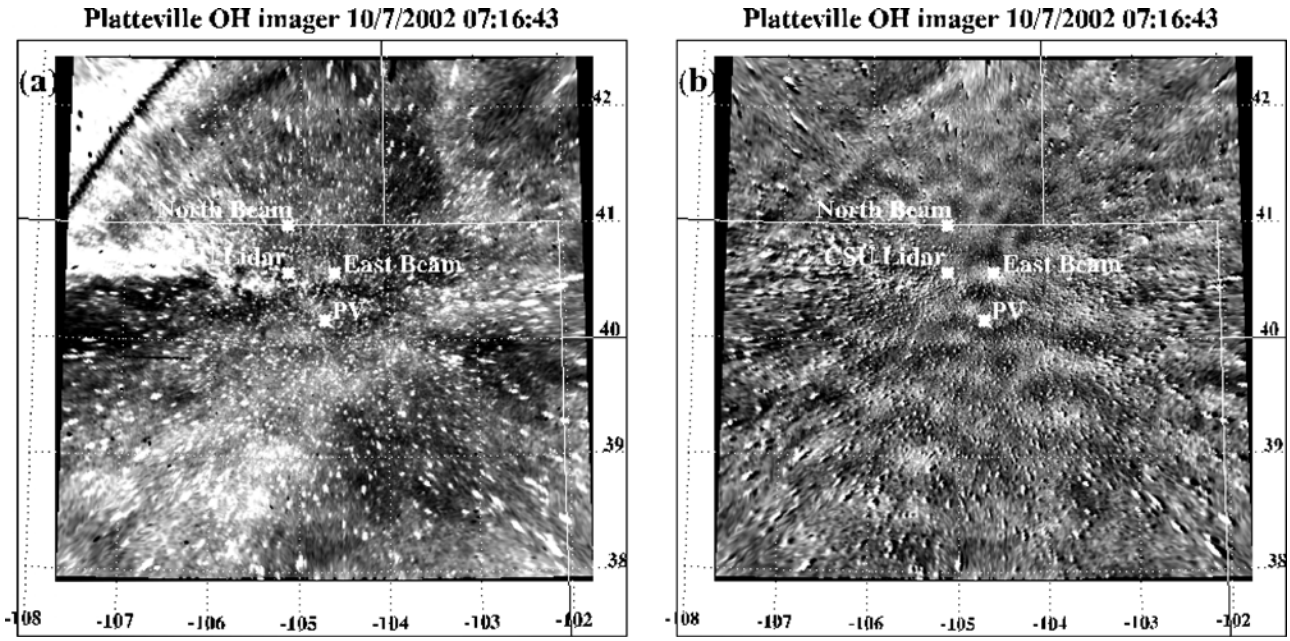

Figure 5. OH imager snap shots at 0717 UT: (a) the normalized raw image and (b) the difference image. Both show the dark bore front in the northwest quadrant. The black line near the northwest edge in Figure 5a is the projection of a power line, thus not seen in Figure 5b.

6/7 October 2002. These contours are based on the respective 30-min averaged profiles. Figure 4d gives plots of Richardson number profiles at 0645, 0715 and 0745,UT. Cloudy conditions between 2.5 and 5.0,UT, made optical observation impossible. Nonetheless, the presence of a brief observation at ~2.0,UT suggests that temperature inversion exists at the OH layer height through out most of the night, certainly between 0200 and 0900,UT, as can be seen in Figure 4a. In Figure 4b, we show coaligned wind speed along the direction of bore propagation. From the descending phase front in the temperature contour, Figure 4a, it is clear that the temperature inversion is related to a long-period wave, likely a semidiurnal tide. The existence of such a wave can also be seen in the contours of Figure 4b. The amplitude of the wave is approximately ~30 K, and ~40 m/s, respectively. In fact, the wave structures between Figures 4a and 4b are generally the same, suggesting tidal effect on inversion layers [*Dao et al.*, 1995; *Meriwether and Gardner*, 2000; *Huang et al.*, 1998] and hence on bore propagation. Since temperature inversions and semidiurnal tides of this magnitude occur often in the MLT, it is not clear, however, why the occurrence of a bore event is relatively rare. Perhaps additional criteria on atmospheric conditions are required for the formation of a mesospheric bore. As an alternative, the relatively infrequent occurrence of bores may be related to the relative rarity of the proper generation conditions. In the case we studied here, the bore was observed to propagate against a strong wind. The importance of strong wind in this respect is not clear since unfortunately, there were no horizontal wind measurements made in the two cases previously reported. More cases of concurrent lidar/imager studies hopefully would help to resolve this puzzle. We also noticed an upward kink near 87 km and 0600UT in the wind contours, Figure 4b, while there is only a mild tem re increase at the same altitude and time in Figure 4a. This kink corresponds to the "hydraulic jump" with an decrease in wind speed. The observed mild temperature increase reflects the expected temperature rise of about 3 K as the bore passes that can be estimated from height change (10 K/km). We can better determine this temperature rise from the observed profiles, Figure 3a, to be 4 ± 1.4 K at 87 km as mentioned earlier.

[16] Unlike the previous bore events, the undulations of the FC/P bore began to disintegrate at ~0653 UT, to develop turbulence at ~0710, and to disappear all together at ~0731 as indicated by OH imager snap shots, Figure 2. Yet the temperature inversion clearly exists in the OH layer during all these times, see Figure 4a. That the destruction of the bore's undulations may be correlated with the onset of dynamic (shear) instability developed between 0645 and 0730,UT, can also be investigated by lidar observation. The wind gradient magnitude in this time interval is seen to increase, as shown in Figure 4c, suggesting dynamical instability. To verify this possibility, we plot the Richardson number profiles at 0645, 0715 and 0745,UT. Indeed, the Richardson profiles at 0645 and 0715 clearly go below 0.25 near 89 km, at the same time the wave train became unstable and disintegrated into the turbulent motion. That the atmosphere during this time period is dynamically unstable is also supported by the observation of the short wavelength ripple-type structure between 0712 and 0727 UT. The ripple structure moved at a speed of ~40 m/s, 30 deg north of east, consistent with lidar measured wind around 87 km. At 0717 UT, as shown in Figure 5b, such a ripple structure is clearly seen near 100 km east of the location (point) marked "CSU lidar." The spatial extent of this structure is about 50 km wide and 100 km long with wavelength ~11 km and phase front aligned along the southwest direction. Taking the thickness of the unstable wind shear layer centered ~88.5 km from Figure 4d at

0715 UT to be 1.5 km, the ratio of ripple wavelength to layer thickness is ~7.3, consistent with K.H. billows. The expected ratio depends on, but is not sensitive to, the exact wind shear profile; it ranges from 6.3 to 7.5 for most shear instabilities [*Turner*, 1973]. It is thus possible that the bore was transformed into a turbulent or foaming bore, as suggested by the theory of *Lighthill* [1978] and of *Dewan and Picard* [1998], losing energy by generating turbulence instead of shedding waves. In this view, the instability is an intrinsic part of the bore development rather than a simple footnote. This would then be the first observation of a mesospheric undular bore in transition to a turbulent bore.

[17] Shown in Figure 5a is the flat-fielded view raw OH image at 0717 UT, with image intensity normalized to hourly mean intensity. Comparing to the corresponding difference image, one can see the bore front in the northwest quadrant in both normalized raw and difference images. The additional black line near the northwest corner of Figure 5a is the projection of a power line; it disappeared in the difference image as expected. However, the ripple structure and chaotic (or foaming) wave segments behind the bore front can only be seen in the difference image. The bore observed by the OH imager appears to be a dark bore, i.e., decrease in brightness following the bore front, as can be seen in all images in Figure 2 with care. This decrease in brightness, which is clearly revealed in both enlarged images shown in Figure 5, suggests that the main duct is below the peak of the OH layer [*Taylor et al.*, 1995; *Dewan and Picard*, 1998], as verified by the lidar N^2 profile in Figure 3b.

5. Conclusion

[18] We reported the observation of an undular bore by an OH imager, located in the Fort Collins/Platteville (FC/P) area on the night of 6/7 October 2002. Unlike the earlier observations, a Na lidar capable of measuring mesopause region temperature, zonal and meridional winds was in operation concurrently. The lidar data confirm, for the first time, the existence of a concurrent, collocated temperature inversion layer which serves as the ducting region for bore propagation, as required by the simple theory proposed by Dewan and Picard six years ago. In addition, the available lidar permitted the determination of the wind speeds in the direction of bore propagation ahead of and behind the bore disturbances. This information coupled with the observed temperature inversion layer can be used, in principle, to determine the undisturbed thickness h_0 of the ducting region and the bore amplitude $h_1 - h_0$. This allows one to deduce all parameters of the bore according to simple theory of Dewan and Picard, without needing other information.

[19] The parameters so determined for the 2002 FC/P bore are compared to the 1993 Hawaii bore and the 1999 MDO bore. Like the other cases, the horizontal wavelength of the FC/P bore estimated from the theory is in good agreement with the observed value and the simple theory appeared to describe the observation well. The lifetime of the FC/P undular bore was however considerably shorter than the other two. Following the evolution of clean undulations, the total observed life of the FC/P undular bore was only about 12 from observed cradle to grave, suggesting the need for a theory describing the transient behavior of bore creation and destruction.

[20] As anticipated, the lidar data can be used to shed more light on the bore dynamics. For example, as reflected from the time-altitude contours of temperature and wind speed along the bore propagation direction, one finds that the evolution of the ducting region (temperature inversion as well as extreme wind speed) is controlled by a long-period wave, likely connected with the semidiurnal tide. Also, the lidar data, enhanced by the observation of KH billows, suggest, for the first time, that atmospheric dynamic instability is associated with the destruction of undulation wave train of a bore. It is also possible that this is the first observation of the transition of an undular mesospheric bore to a turbulent bore. With more concurrent lidar/imager observation of bore events, one may be able to answer the presently open question: Why do so many mesospheric temperature inversion layers exist without the presence of bores?

[21] **Acknowledgments.** The authors express their heartfelt thanks to Edmond Dewan for his guidance for and enthusiastic encouragement during this study. This work is supported in part by grants from National Aeronautics and Space Administration, NAG5-10076, and from National Science Foundation, ATM-00-03171, and ATM-0137555.

References

Dao, P. D., R. Farley, X. Tao, and C. S. Gardner (1995), Vertical structure of the midlatitude temperature from stratosphere to mesosphere (30–105 km), *Geophys. Res. Lett.*, *22*, 2825–2828.

Dewan, E. M., and R. H. Picard (1998), Mesospheric bores, *J. Geophys. Res.*, *103*, 6295–6305.

Dewan, E. M., and R. H. Picard (2001), The origin of mesospheric bores, *J. Geophys. Res.*, *106*, 2921–2927.

Huang, T.-Y., T.-F. Tuan, X. Li, E. M. Dewan, and R. H. Picard (1998), Sudden narrow temperature inversion-layer formation in ALOHA 93 as a critical-layer-interaction phenomenon, *J. Geophys. Res.*, *103*, 6323–6332.

Huang, T.-Y., M. P. Hickey, T.-F. Tuan, E. M. Dewan, and R. H. Picard (2002), Further investigations of a mesospheric inversion layer observed in the ALOHA-93 Campaign, *J. Geophys. Res.*, *107*(D19), 4408, doi:10.1029/2001JD001186.

Lighthill, J. (1978), *Waves in Fluids*, Cambridge Univ. Press, New York.

Meriwether, J., and C. S. Gardner (2000), A review of the mesosphere inversion layer phenomenon, *J. Geophys. Res.*, *105*, 12,405–12,416.

Peterson, A. W., and L. M. Kieffaber (1973), Infrared photography of OH airglow structure, *Nature*, *224*, 92.

She, C.-Y. (2004), Initial full-diurnal-cycle mesopause region lidar observations: Diurnal-means and tidal perturbations of temperature and winds over Fort Collins, CO (41N, 105W), PSMOS 2002, *J. Atmos. Sol. Terr. Phys.*, *66*, 663–674.

She, C. Y., and R. P. Lowe (1998), Seasonal temperature variations in the mesopause region at mid-latitude: Comparison of lidar and hydroxyl rotational temperatures using WINDII/UARD OH height profiles, *J. Atmos. Sol. Terr. Phys.*, *60*, 1573–1583.

Smith, S. M., M. J. Taylor, G. R. Swenson, C. She, W. Hocking, J. Baumgardner, and M. Mendillo (2003), A multidiagnostic investigation of the mesospheric bore phenomenon, *J. Geophys. Res.*, *108*(A2), 1083, doi:10.1029/2002JA009500.

Taylor, M. J., D. N. Turnbill, and R. P. Lowe (1995), Spectrometric and imaging measurements of a spectacular gravity wave event observed during the ALOHA-93 campaign, *Geophys. Res. Lett.*, *22*, 2849–2852.

Turner, J. S. (1973), *Buoyancy Effects in Fluids*, Cambridge Univ. Press, New York.

T. Li, C. Y. She, B. P. Williams, and T. Yuan, Department of Physics, Colorado State University, Fort Collins, CO 80523, USA. (joeshe@lamar.colostate.edu)

R. H. Picard, Air Force Research Laboratory, Hanscom AFB, MA 01731, USA.

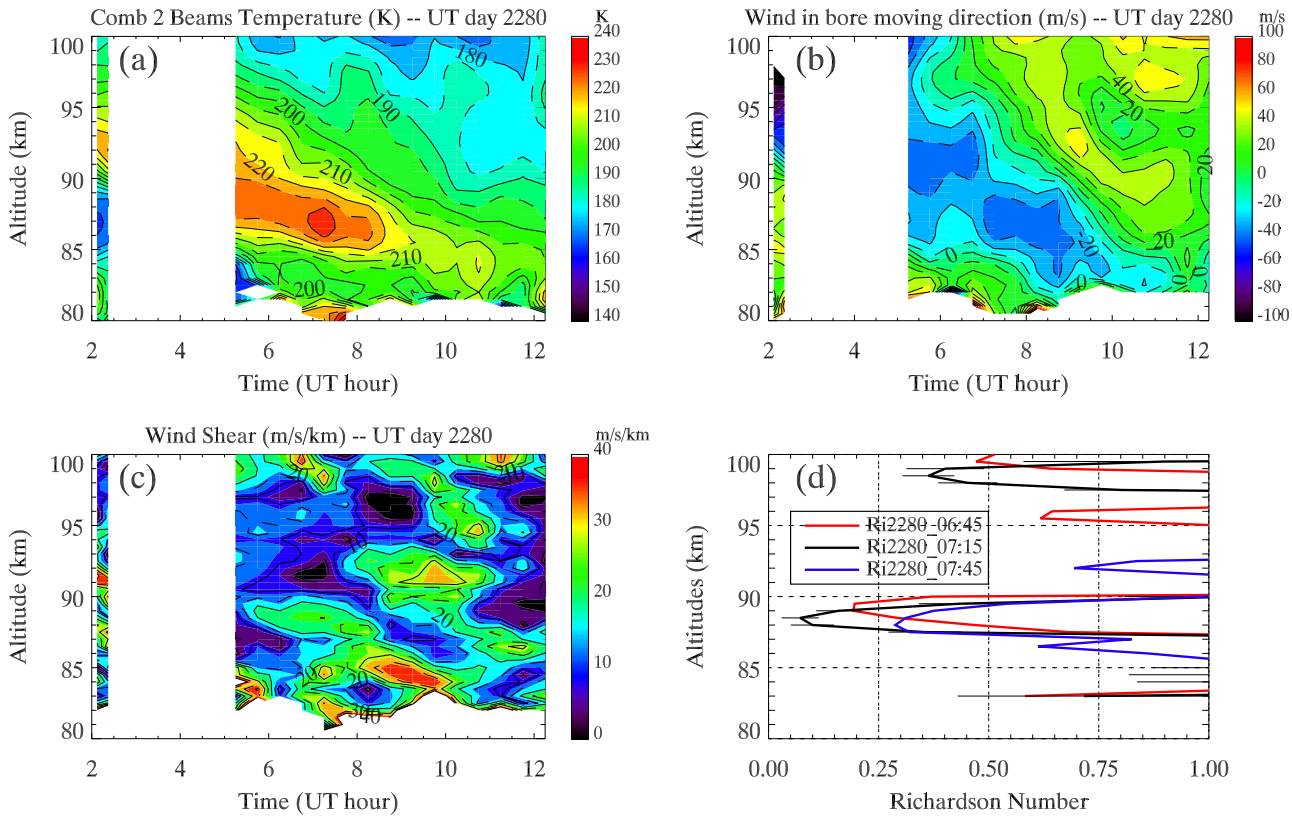

Figure 4. Contour plots of (a) temperature, (b) wind speed along bore propagation direction, and (c) the magnitude of vertical gradient of horizontal wind throughout the night of 6/7 October 2002. These contours are based on respective 30-min averages profiles. (d) Plots of Richardson number profiles at 30-min interval centered at different times.